DEUTSCHES ELEKTRONEN-SYNCHROTRON **DESY**

DESY 80/75
Bonn-HE-80-5
July 1980

TWO PHOTON RESULTS FROM TASSO

TASSO - Collaboration

presented by E. Hilger
Physikalisches Institut der Universität Bonn

NOTKESTRASSE 85 · 2 HAMBURG 52

To be sure that your preprints are promptly included in the
HIGH ENERGY PHYSICS INDEX ,
send them to the following address (if possible by air mail) :

DESY
Bibliothek
Notkestrasse 85
2 Hamburg 52
Germany

TWO PHOTON RESULTS FROM TASSO *)

TASSO Collaboration

Aachen, Bonn, DESY, Hamburg, Imperial College, Rutherford, Oxford, Weizmann, Wisconsin [1)]

presented by E. Hilger,
Physikalisches Institut der Universität Bonn, Nussallee 12, D-5300 Bonn 1

Summary

Two photon interactions were observed with the TASSO detector at the e^+e^- storage ring PETRA. We report on the analyses of two-prong and multiprong events.
Both no-tag and single-tag events with a two-prong final state seen in the central detector are selected and compared to the expectations from two-photon QED processes. In the no-tag data we observe a good agreement, except for a pronounced excess of events in the invariant mass range around the f^o mass. We quote a preliminary value for the radiative decay width of the f^o of $\Gamma(f^o \to \gamma\gamma) = 4.1 \pm 0.4$ keV with 15% systematic uncertainty.
Multihadronic events are observed in the single tag mode and interpreted in the spirit of vector dominance ideas. From an overall fit to the measured distributions of transverse momenta, charged multiplicities, and visible energies we derive total cross sections for hadron production as a function of the center-of-mass energy of the two photon system.

*) enlarged version of a talk given at the International Workshop on $\gamma\gamma$ Collisions, Amiens, April 8-12,1980, France.

Early work on photon-photon scattering began in the mid thirties /2/. Then for about twenty-five years the subject went dormant before the relevance of two-photon physics was recognized in 1960 /3/. Its definitive revival came about ten years later /4/. Nowadays an ever rising interest in two-photon processes can be observed at the high energy e^+e^- storage rings.
At PETRA the TASSO experiment, for which the study of two photon collisions so far was not among the top priority issues on the physics menu, lately has increased its efforts in this field.

This is a report on the status of the investigations in two photon physics at TASSO. It is based on data taken in the fall of 1979 at beam energies around 15 GeV, in part also on data taken in 1980 at beam energies up to 17.6 GeV. Analysis is still in progress and most of the results reported here are preliminary.

The two photon mechanism at e^+e^- machines is illustrated in fig. 1. The process observed in the experiment is of the type

$$e^+e^- \longrightarrow e^+e^- + X, \qquad (1)$$

which is related in a non-trivial way /5,6/ to the genuine two photon reaction

$$\gamma\gamma \longrightarrow X, \qquad (2)$$

where X is any produced particle system of invariant mass M_X.

In this report we will discuss two classes of two photon processes. In the first part the system X will consist of just two charged particles. The QED processes of the production of charged lepton pairs belong to this class as well as the two photon production of a resonance which subsequently decays in two charged particles. The second part of this report will be devoted to events with X being a multihadronic system of at least three particles. From these we have obtained total cross sections for two photon production of hadrons.

A specific signature of reaction (1) is the occurrence of an electron and a positron in the final state, both peaked at high energies and extreme forward angles. Also distinctly different from the one photon annihilation processes is the distribution of the total energy of the produced system X. For two photon events this distribution rises steeply toward zero energy while for annihilation events it peaks in principle at twice the beam energy. Both characteristic features are used in TASSO to select $\gamma\gamma$ reactions.

Fig. 2 shows a cut through the TASSO detector along the beam axis. The central part consists of a large magnetic solenoid, the volume of which is filled with tracking chambers, a cylindrical proportional chamber surrounded by a cylindrical drift chamber /7/, and scintillation counters used in the trigger and to measure time of flight. Just this inner part, details of which can be found in /8/, was used in the present study of particle systems X produced in two photon collisions.
On either side of the central part further out along the beam pipe there are forward detectors. They measure the luminosity and allow to detect the scattered electrons and positrons from two photon processes. Fig. 3 is a view on one of the forward detectors along the beam axis. A hodoscope for charged particles consists of 16 scintillation counters covering forward angles between 24 mrad and 60 mrad. In TASSO the detection of tag-particles is restricted to this angular range by the hole in the end cap yoke of the main detector and by the size of the beam pipe. An array of 36 lead glass shower counters behind the hodoscope measures the energy of electrons and photons. The thickness of these counters is about 12 radiation lengths.

At present the study of two photon processes with TASSO follows two separate roads.
In one analysis the events with no tag-particles observed are used and two photon candidates are selected mainly on the basis of their measured total energy. These events predominantly come from scattering of almost real photons.

The other analysis considers the events with a single tag in one of the forward detectors. Due to the restricted angular acceptance the tagged photon has a rather small but finite four momentum Q^2 while the untagged photon again almost always is real.

The analysis of the untagged events will be described first. No special hardware trigger exists for untagged two photon events. But the standard triggers for 1γ-reactions also accept two photon induced events.
One of these triggers, used for the analysis presented here, was a pair trigger. It demanded two or three charged tracks coplanar with the beam axis to within 27° having a minimum momentum transverse to the beam of about 0.3 GeV/c. The pair trigger covered azimuthal angles between 0 and 2π and polar angles between 35° and 145°.
Two photon induced two prong events were selected in two steps requiring at first two tracks, which originated from the interaction region, were oppositely charged, coplanar to less than 10°, and had a time of flight difference of less than 5 ns. These cuts effectively removed all background from cosmic rays and beam gas scattering.
Then in a second step two-prong events originating from one-photon processes being mainly lepton pairs were rejected by requiring the two tracks to be non-collinear by more than 5° and the sum of their momenta to be less than 20% of the total energy available in the e^+e^- collision.

The effect of the latter cut is illustrated with fig. 4 which shows the distribution of x, where x is the sum of the track momenta in each event normalized to the available energy in the e^+e^- system. The indicated cut in x eliminates the remainder of one-photon events surviving the collinearity cut; these events peak around x = 1 and are attributed to radiative lepton pair production.
For the events below the x-cut we plot in fig. 5 the modulus of the vector sum of the transverse momenta $|\vec{p}_{T_1} + \vec{p}_{T_2}|$. The plot demonstrates that the transverse momenta of the two tracks are balanced.

This, together with the steeply falling x-distribution from fig. 4, allows to conclude that these events originate from two-photon production of a pair of charged particles.

A total of 3335 events passing the selection criteria were found for an integrated luminosity of 4109 nb^{-1} taken at beam energies ranging from 13.7 GeV to 17.6 GeV.

In fig. 6 we plot the p_T-distribution of the individual tracks in these events. The curve is the prediction for continuum pair production. The dominant part of this comes from lepton pair production in two photon interactions

$$e^+e^- \rightarrow e^+e^- + L^+L^-, \qquad L^+L^- = (e^+e^-, \mu^+\mu^-). \qquad (3)$$

These processes were simulated in the detector using the event generator written by J.A.M. Vermaseren /9/. For the measured total luminosity electron pair and muon pair production were computed separately. Two-photon production of pion pairs is small compared to lepton pair production, however favored by the acceptance of the detector. The Born term contribution from pion pair production, which is likely to be an overestimate, was calculated using a computer program written by Krasemann and Vermaseren /10/ and was found to contribute roughly 16% to the continuum pair production.

Fig. 7 shows the distribution of the invariant mass M_X of the two prongs assigning pion masses to them. In both distributions shown in figs. 6 and 7 we observe a pronounced excess over the QED prediction in a particular region which indicates a considerable contribution from resonance production in the sample.

This conclusion is supported by the angular distributions plotted separately for different M_X regions in fig.8. The angle plotted on the abscissae is the angle between the beam axis and the direction of the observed pairs in their center-of-mass system. Again, for M_X below 1 GeV and above 1.5 GeV the data are well described by the 2γ-QED prediction. But for the M_X interval in between the data by far exceed the expectation from continuum production.

An obvious candidate for the observed resonance is the tensor meson f^o. We simulate the production of f^o mesons in two-photon-interactions with the subsequent decay of the f^o's in $\pi^+\pi^-$ according to a model developed by Krasemann an Vermaseren /10/ using a program provided by these authors. Then we apply a maximum likelihood fit to the observed mass distribution and determine the relative contributions of the f^o and the continuum. As a result of the fit the background is adjusted by a factor o.9 and plotted as such in fig.7. This adjustment is not unreasonable. The systematic error in our data is about 13%, our background includes a contribution from continuum pion pair production which may be largely overestimated, and effects of radiative corrections are not included.

In fig. 9 we plot the difference between the data and the background from fig. 7. In the mass range of the f^o a magnificent signal is observed. The curve shown is the fit result for the f^o contribution. From this we calculate a width for the decay $f^o \rightarrow 2\gamma$. We obtain a preliminary value of $\Gamma(f^o \rightarrow \gamma\gamma) = 4.1 \pm o.4$ keV, with an additional systematic uncertainty of $\pm$ 15%. The observed width of the signal of about 200 MeV supports our assumption that any contribution from a broad ($\gtrsim$300 MeV) scalar resonance like the $\epsilon(1300)$ must be very small.

In fig. 10 we compare our result with the recent measurement from the PLUTO collaboration /11/ and the theoretical predictions /12/ published since the discovery of the f^o in 1962.

We now turn to the analysis of the events with a single tag in the forward detector.

Candidates for two photon induced events were selected by a special trigger which demanded an energy of more than 3.5 GeV deposited by a charged particle in one of the forward detectors and at least one track with a momentum transverse to the beam exceeding 0.3 GeV/c in the central detector.

The off-line selection required at least one track fully reconstructed in space and at least one more track reconstructed in two dimensions (r,ϕ). That reduced the roughly 180 000 triggers to 2125 events, which then were scanned by inspection on a graphics terminal. Track pairs from converted photons were removed and obvious background events rejected.

The analysis procedure now was split up in two branches.
In order to isolate events from two photon production of lepton pairs (3) events with just two tracks in the central detector were separated. The two tracks were required to balance in charge and their common vertex had to lie within $\Delta z = \pm 7.5$ cm off the nominal interaction point, where z is the coordinate along the beam. The two tracks had to be coplanar to within 45°.
These cuts reduced the background from beam gas scattering and from multihadronic final states to less than 8 % each.

After background subtraction the final data sample contained 649 candidate events for reaction (3), collected for a total luminosity of 2040 nb^{-1} at beam energies between 14.95 GeV and 15.73 GeV.
Fig. 11 shows an especially remarkable event from this sample since it is one of the rare specimens with a double tag. The upper half of the figure shows the event in the central detector in three views, the lower half shows the hits and deposited energies in the forward detectors. From the insets one can tell that the two track system is boosted toward +z (EAST), where the tag particle had a lower energy than the one found in the WEST detector.

In the following three figures the data are compared to the absolute expectation for two photon production of charged lepton pairs. The predicted distributions were calculated using again the exact treatment of the matrix element by J.A.M. Vermaseren /9/ in a Monte Carlo simulation of the acceptance and the offline selection. In fig. 12a the distribution of p_T is shown, where p_T is the momentum of a track transverse to the beam axis, while fig. 12b shows this transverse momentum squared. In fig. 13 we plot the invariant mass distribution of the events assigning pion masses to the tracks.
In all three plots the data agree well to the absolute expectation from two-photon QED processes proving that event selection and acceptance calculation are properly understood.

The invariant mass plot for the single tag two prongs does not show much evidence for the f^o meson. This we view as a consequence of the mean Q^2 of the tagged photon being 0.26 GeV^2. This finite Q^2 results in a suppression of f^o production.

The second branch of the analysis of single tag events concerned the production of multihadronic final states in two-photon scattering.
Out of the 2125 preselected single tag events mentioned above candidates for the reaction

$$e^+e^- \longrightarrow e^+e^- + \text{hadrons} \qquad (4)$$

were selected requiring at least three tracks in the central detector. Two of these had to be fully reconstructed in space and one more reconstructed in two dimensions (r,ϕ), and not all three tracks were allowed to have the same charge sign.
Fig. 14 shows a vertex distribution of the events satisfying these conditions. A cut at $z = \pm 7.5$ cm left a background from beam gas events of about 12% in the sample which had to be subtracted statistically.
Fig. 15 presents one event from the final data sample containing 397 events collected for an integrated luminosity of 2280 nb^{-1} at beam energies between 13.7 and 15.73 GeV.
Fig. 16 shows the observed distribution of p_T^2, the squared momentum transverse to the beam axis, on a logarithmic plot. For small p_T^2 up to about 1 $(GeV/c)^2$ the data show an exact exponential fall-off with a slope factor of -5 $(GeV/c)^{-2}$. Above 1 $(GeV/c)^2$ we observe an excess over this steep fall-off, which may indicate a contribution to process (4) from a pointlike coupling of the photon, but may be at least partially also attributed to other sources.

We have simulated the process (4) in the TASSO detector with Monte Carlo methods.
In order to extract cross sections for the reaction

$$\gamma\gamma \rightarrow \text{hadrons} \qquad (5)$$

from the measured data we followed the concept of two-photon luminosity functions as recently discussed by Field /6/.

This approach avoids the kinematical approximations of the Weizsäcker-Williams (EPA) formulae /5/. As a consequence, for low z, $z = W_{\gamma\gamma}/2 \cdot E_{beam}$, the photon-photon luminosity comes out considerably higher than in the EPA.

The cross section for reaction (5) was parameterized in the spirit of VDM ideas /13/ including a form factor ansatz for the virtual photons:

$$\sigma(W_{\gamma\gamma};\ Q_1^2, Q_2^2) = (A + B/W_{\gamma\gamma}) \cdot \left[\frac{1}{1 + Q_1^2/m_\varrho^2}\right]^2 \cdot \left[\frac{1}{1 + Q_2^2/m_\varrho^2}\right]^2 \qquad (6)$$

The hadronic system was generated according to a multipion phase space model with limited transverse momentum relative to the photon-photon axis,

$$\langle p_T^{\gamma\gamma} \rangle = C, \qquad (7)$$

and a ratio of charged to neutral particles of 2:1.
The mean charged multiplicity was assumed to be linear in $\ln W_{\gamma\gamma}$ and parameterized as

$$\langle n_{ch} \rangle = D + E \cdot \ln W_{\gamma\gamma}. \qquad (8)$$

The events generated according to this model were subjected to the acceptance of the detector, the trigger conditions, the efficiencies of the trigger and the track reconstruction, and the offline cuts.
The resulting distributions of observable quantities were compared to the data. The five parameters A to E were simultaneously fitted to three measured distributions, the squared momentum transverse to the beam axis [but only up to 0.9 $(GeV/c)^2$], the charged multiplicity, and the visible energy.
In an iterative procedure the χ^2 was minimized in the five parameter space. A minimum was found for the following set of parameters

$$\begin{aligned} \langle p_T^{\gamma\gamma} \rangle &= 0.298 \text{ GeV/c} \\ \langle n_{ch} \rangle &= 2.1 + 1.5 \ln W_{\gamma\gamma}(GeV) \\ \sigma_{\gamma\gamma \to had}(W_{\gamma\gamma};\ q_1^2 = q_2^2 = 0) &= 380 + 520/\ W_{\gamma\gamma}(GeV) \text{ nb.} \end{aligned} \qquad (9)$$

The corresponding χ^2 values, both individual and total, were reasonably small, e. g.

$$\chi^2_{\text{total}}/\text{d.o.fr.} = 1.05. \qquad (10)$$

The result of the Monte Carlo simulation with the optimized set of parameters is also shown in fig. 16 and in the following figures. In a check the excess at p_T^2 larger than 1 $(GeV/c)^2$ has been put in our present model in a purely phenomenological ansatz. We found that the parameters are only slightly modified such that the total cross section is affected by little over 5 %.

The observed distribution of the charged multiplicity for the reaction $e^+e^- \to e^+e^-$ + hadrons (4) is presented in fig. 17. The agreement between data and simulation is very good.

Using our optimized set of parameters we are able to extract information directly on the two photon production process of hadrons.
We have plotted in fig. 18 the mean charged multiplicity for $\gamma\gamma \longrightarrow$ hadrons (5). The central line represents the result of the best fit $\langle n_{ch} \rangle = 2.1 + 1.5 \cdot \ln W_{\gamma\gamma}$, and the hatched area indicates the range up to ± 1 standard deviation as obtained by a careful analysis of the statistical errors in the five parameter space. There is an additional systematic uncertainty in each parameter estimated to be less than ± 15%.
For comparison we have indicated also the mean charged multiplicities in other processes of hadron production, for one photon annihilation taken from a recent fit /14/ to all data with center-of-mass energies between 1.4 and 32 GeV, as well as the corresponding curves for $\bar{p}p$ annihilation /15/ and pp scattering /16/.

In fig. 19 we show the measured distribution of visible energies. Again we find that our simple model described above fits our data quite well with the set of parameters given in (9). With these parameters we obtain the hadronic cross section for scattering of two real photons at center-of-mass energies between about 2 and 9 GeV, as plotted in fig. 20. The central line corresponds to a functional dependence of the extrapolated cross section on the two photon energy of

$$\sigma(W_{\gamma\gamma}; 0,0) = 380 + \frac{520}{W_{\gamma\gamma}(\mathrm{GeV})} \text{ nb.} \qquad (11)$$

In addition to the statistical error indicated in the figure there is a systematic uncertainty in each parameter at present estimated to be less than ± 25%.

We believe we have demonstrated that our approach of an overall fit to the measured distributions of the reaction $e^+e^- \longrightarrow e^+e^-$ + hadrons allows to extract information on hadron production in two photon scattering within reasonable errors. This analysis represents the first attempt to obtain detector independent results on two photon production of hadrons.

Acknowledgement

I am grateful to my colleagues in the TASSO collaboration for numerous discussions, in particular to W. Hillen, H. Kolanoski, P. Leu, H.U. Martyn, M. Wollstadt, and R.J. Wedemeyer. I want to thank Prof. P. Kessler for the invitation and Prof. G. Cochard and the organizers of the Amiens Workshop for a most enjoyable meeting.

References

/1/ The present members of the TASSO collaboration are
R. Brandelik, W. Braunschweig, K. Gather, V. Kadansky, K. Lübelsmeyer, P. Mättig, H.-U. Martyn, G. Peise, J. Rimkus, H.G. Sander, D. Schmitz, A. Schultz von Dratzig, D. Trines, W. Wallraff,
I. Physikalisches Institut der RWTH Aachen, Germany;
H. Boerner, H.M. Fischer, H. Hartmann, E. Hilger, W. Hillen, L. Koepke, H. Kolanoski, G. Knop, P. Leu, B. Löhr, R. Wedemeyer, N. Wermes, M. Wollstadt,
Physikalisches Institut der Universität Bonn, Germany;
H. Burkhardt, D.G. Cassel, D. Heyland, H. Hultschig, P. Joos, W. Koch, P. Koehler, U. Kötz, H. Kowalski, A. Ladage, D. Lüke, H.L. Lynch, G. Mikenberg, D. Notz, J. Pyrlik, R. Riethmüller, M. Schliwa, P. Söding, B.H. Wiik, G. Wolf,
Deutsches Elektronen-Synchrotron DESY, Hamburg, Germany;
R. Fohrmann, M. Holder, G. Poelz, O. Römer, R. Rüsch, P. Schmüser,
II. Institut für Experimentalphysik der Univ. Hamburg, Germany;
D.M. Binnie, P.J. Dornan, N.A. Downie, D.A. Garbutt, W.G. Jones, S.L. Lloyd, D. Pandoulas, J. Sedgbeer, S. Yarker, C. Youngman,
Department of Physics, Imperial College London, England;
R.J. Barlow, I. Brock, R.J. Cashmore, R. Devenish, P. Grossmann, J. Illingworth, M. Ogg, B. Roe, G.L. Salmon, T. Wyatt,
Department of Nuclear Physics, Oxford University, England;
K.W. Bell, B. Foster, J.C. Hart, J. Proudfoot, D.R. Quarrie, D.H. Saxon, P.L. Woodworth,
Rutherford Laboratory, Chilton, England;
Y. Eisenberg, U. Karshon, D. Revel, E. Ronat, A. Shapira,
Weizmann Institut, Rehovot, Israel;
J. Freemann, P. Lecomte, T. Meyer, Sau Lan Wu, G. Zobernig,
Department of Physics, University of Wisconsin, Madison, Wisconsin, USA;

/2/ L.D. Landau, E.M. Lifschitz, Sov. Phys. 6 (1934) 244

/3/ F.E. Low, Phys. Rev. 120 (1960) 582;
F. Calogero and C. Zemach, Phys. Rev. 120 (1960) 1860

/4/ A. Jaccarini, N. Arteaga-Romero, J. Parisi and P. Kessler, Compt. Rend. 269B (1969) 153, 1129;
Nuovo Cimento 4 (1970) 933;
V.E. Balakin, V.M. Budnev and I.F. Ginzburg, Zh.E.T.F. Pis'ma 11 (1970) 559 (JETP Lett.II, 388);
S. Brodsky, T. Kinoshita and H. Terazawa, Phys. Rev. Lett. 25 (1970) 972; Phys. Rev. D4 (1971) 1532;
H. Terazawa, Rev. Mod. Phys. 45 (1973) 615

/5/ A. Carimalo, P. Kessler and J. Parisi,
Phys. Rev. D20 (1979) 1957; Phys. Rev. D20 (1979) 2170;
Phys. Rev. D21 (1980) 669

/6/ J. Field, DESY 79/78 (1979), to be publ. in Nucl. Phys.

/7/ H. Boerner et al, DESY 80/27 (1980), submitted to Nucl. Instr. and Meth.

/8/ TASSO Collaboration, R. Brandelik et al., Phys. Lett. 83B (1979) 20

/9/ J.A.M. Vermaseren, private communication

/10/ H.Krasemann and J.A.M. Vermaseren, private communication

/11/ PLUTO Collaboration, Chr. Berger et. al., DESY 80/34, to be published in Phys. Lett.

/12/ L.V.Fil'kov, JETP Lett. 5(67)153;
G.M.Radutskii, JETP Lett. 6(67)336; Sov.J.Nucl.Phys.8(69)65;
Kunzst et. al., Dubna Report E2-5424;
B.Renner, Nucl. Phys. B30(71)634;
B.Schrempp-Otto et. al., Phys. Lett. 36B(71)463;
updated 1980, private communication;
A.Bramon et. al., Lett. Nuov. Cimento 2(71)522;
H.Kleinert et. al., Nucl. Phys. B38(72)87;
G.Schierholz et. al., Nucl. Phys. B40(72)125;
St.B.Berger et. al., Phys. Rev. D8(73)3875;
V.N.Novikov et. al., Sov.J.Nucl.Phys. 21(75)529;
D.Faiman et. al., Phys. Lett. 59B(75)269;
N.Levy et. al., Phys. Rev. D13(76)2662;
P.Grassberger et. al., Nucl. Phys. B106(76)451;
J.Babcock et. al., Phys. Rev. D14(76)1286;
M.Greco, Nuovo Cimento 42A(77)315;
M.Greco et. al., Nuovo Cimento 43A(78)88;
V.M.Budnev et. al., Phys. Lett. 86B(79)351;
W.N.Cottingham et. al., J. Phys. G5(79)L155;

/13/ V.N. Gribov and I.Ya. Pomeranchuk, Phys.Rev.Lett. 8(62)343;
Reports of S. Brodsky and T. Walsh in the Proceedings of the Intern. Colloq. on Photon-Photon Collisions, Suppl. au Journal de Physique, Vol 35 C2 (1974)

/14/ TASSO Collaboration, R. Brandelik et al., Phys.Lett. 89B(1980)418

/15/ W. Thome et al., Nucl. Phys. B129 (1977) 365;
see also the review by E. Albini, P. Capiluppi, G. Giacomelli, and R.M. Rossi, Nuovo Cim. 32A (1976) 101

/16/ Data given by R. Stenbacka et al., Nuovo Cimento 51A(1979)63

Figure Captions

Fig. 1: The two photon mechanism in e^+e^- interaction.

Fig. 2: The TASSO detector (cut along the beam axis).

Fig. 3: The TASSO forward detector (view along the beam axis).

Fig. 4: Distribution of the sum of the track momenta per event normalized to twice the beam energy for the background subtracted no tag two prong events. The indicated cut eliminates the remainder of the one photon events surviving the collinearity cut.

Fig. 5: Distribution of $|\vec{p_T} + \vec{p_{T_2}}|$ for the no tag two photon sample of two prong events.

Fig. 6: Distribution of the transverse momenta of the individual tracks for the two photon two prong events (no tag).

Fig. 7: Invariant mass distribution of the candidate events for two photon induced two prongs with no tag observed. This is compared to the expectation for lepton pair production in two photon processes /9/.

Fig. 8: Angular distributions for different invariant mass regions (data and expectation as in fig. 7).

Fig. 9: The f^0 signal obtained from fig. 7 together with the fit of the model /10/.

Fig. 10: Data and predictions on the radiative width $\Gamma(f^0 \to \gamma\gamma)$.

Fig. 11: A double tag event with two charged particles seen in the central detector.

Fig. 12: Distributions of p_T and p_T^2 for candidate events for two photon produced charged lepton pairs with a single tag observed (backgrounds subtracted). The curves are absolute predictions obtained using the event generator written by J.A.M. Vermaseren /9/.

Fig. 13: Invariant mass distribution for the single tag two prong events. The curve is the absolute expectation for two photon produced charged lepton pairs.

Fig. 14: Vertex distribution of the candidates for two photon produced multihadronic final states with a single tag observed.

Fig. 15: Candidate event for $e^+e^- \to e^+e^-$ + hadrons.

Figure Captions (cont'd)

Fig. 16: Distribution of p_T^2 , the squared momentum transverse to the beam axis, for the two photon multihadronic events with a single tag. Also given is the Monte Carlo simulation according to our simplified model described in the text.

Fig. 17: Distribution of the charged multiplicities, observed and simulated.

Fig. 18: Mean charged multiplicity for $\gamma\gamma \rightarrow$ hadrons vs the c.m. energy of the two photon system as obtained from the best fit. The hatched band indicates the range of $\pm$ 1σ in the statistical error. Also indicated are the mean charged multiplicities found in other reactions.

Fig. 19: Distribution of the visible enrgies, both observed and simulated.

Fig. 20: The hadronic cross section for scattering of two real photons vs the c.m. energy of the two photon system as obtained from the fit to our data under the assumptions stated in the text. The hatched area indicates the range of the statistical error.

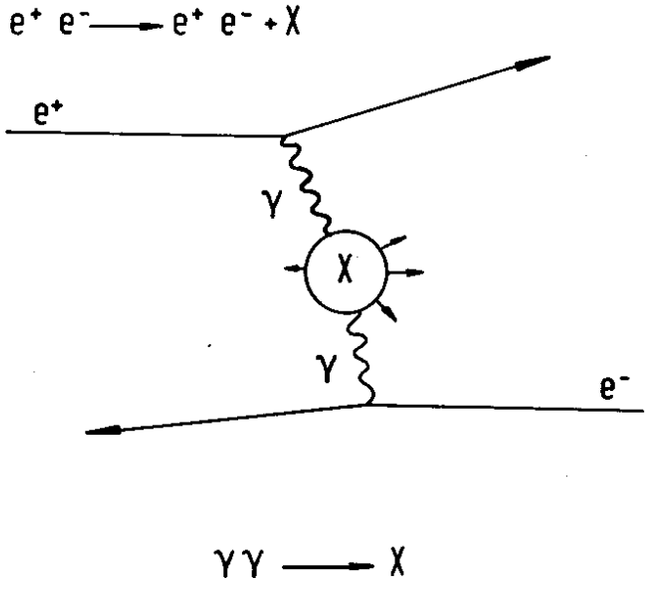

Fig.1

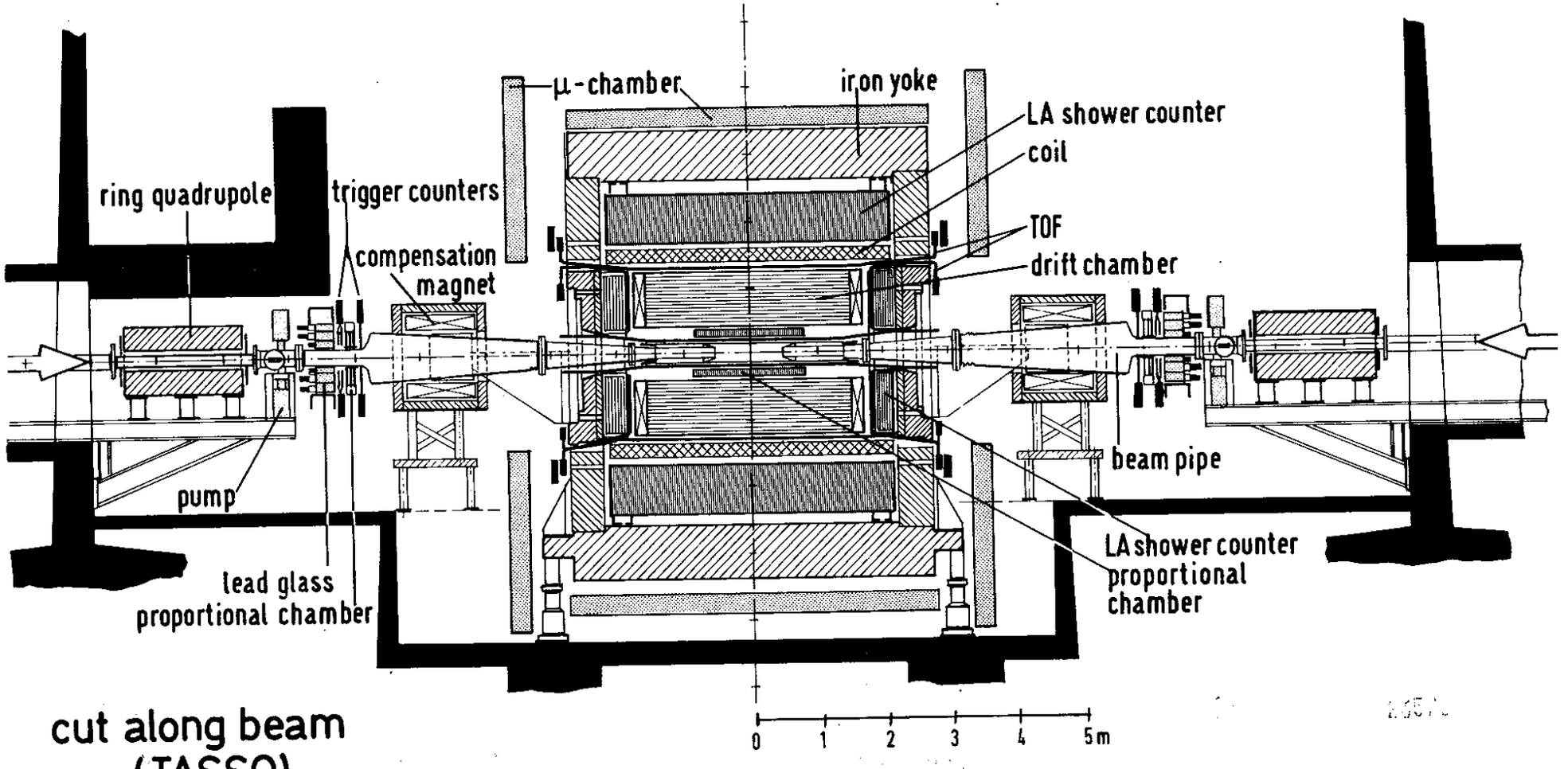

cut along beam
(TASSO)

Fig.2

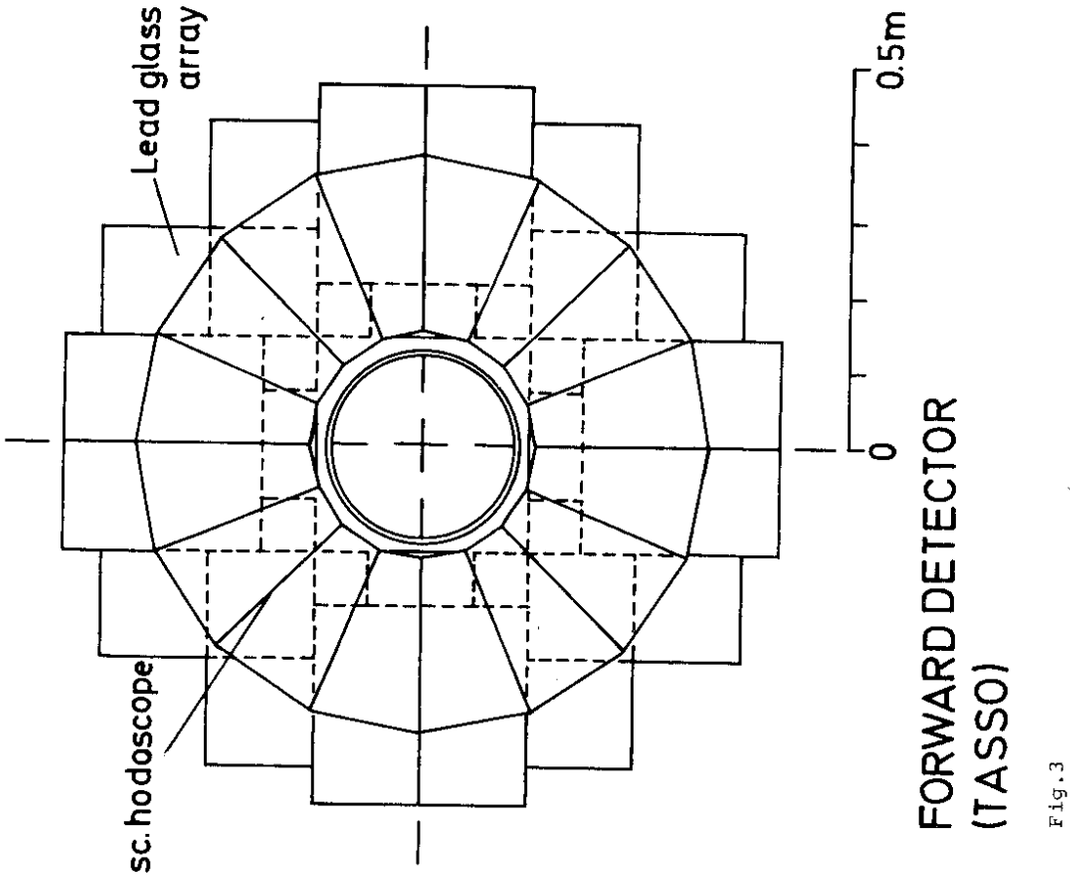

Fig.3

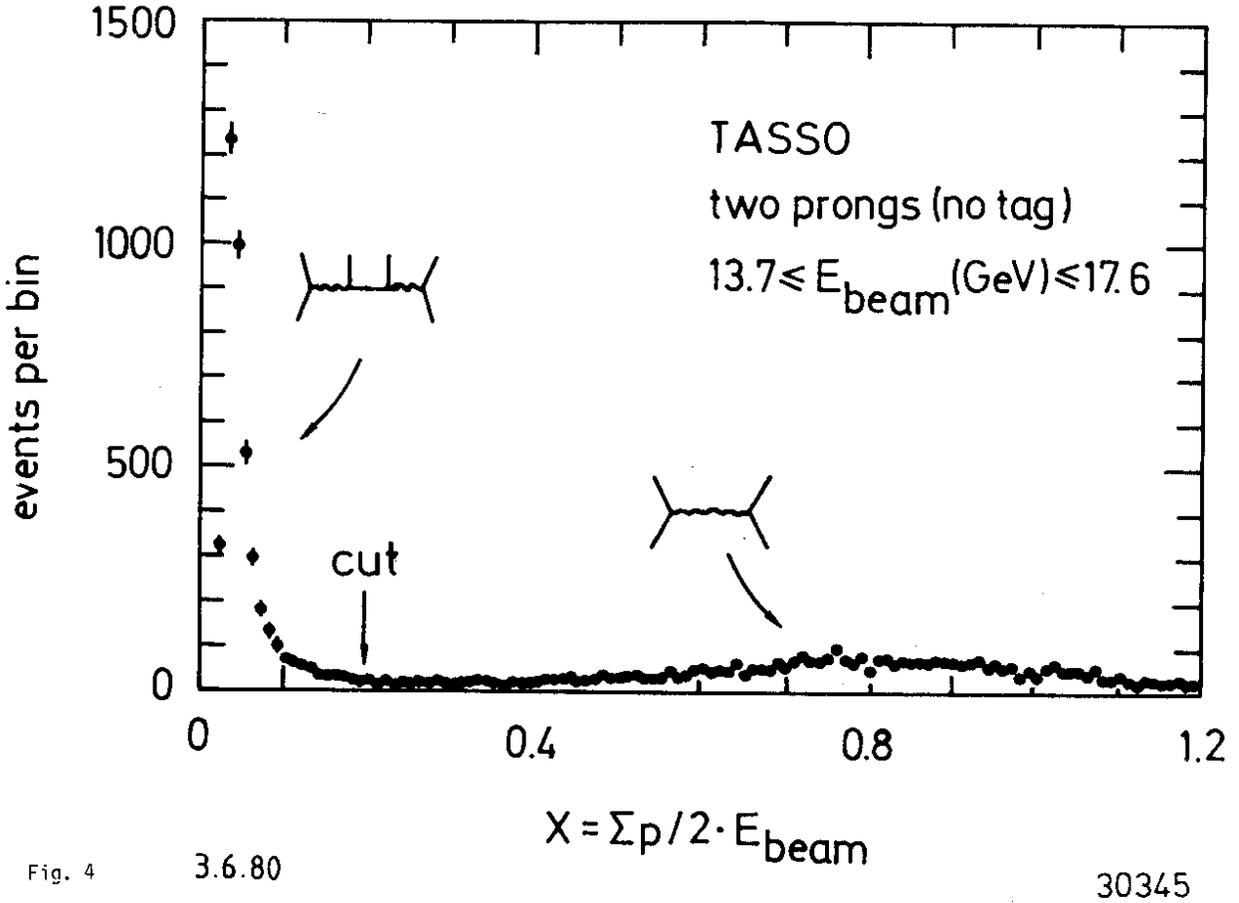

Fig. 4 3.6.80

30345

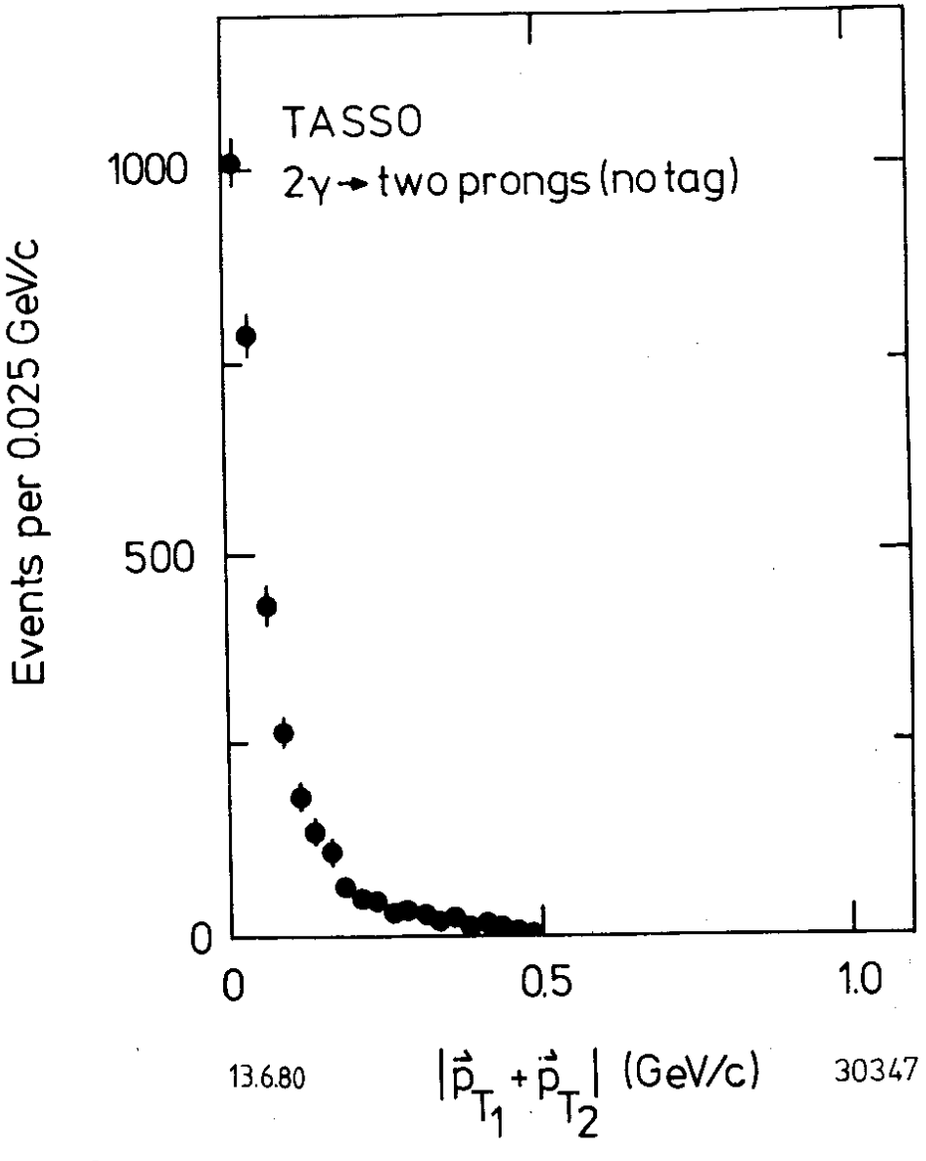
TASSO
2γ → two prongs (no tag)
Events per 0.025 GeV/c
1000
500
0
0
0.5
1.0
13.6.80
$|\vec{p}_{T_1} + \vec{p}_{T_2}|$ (GeV/c)
30347

Fig. 5

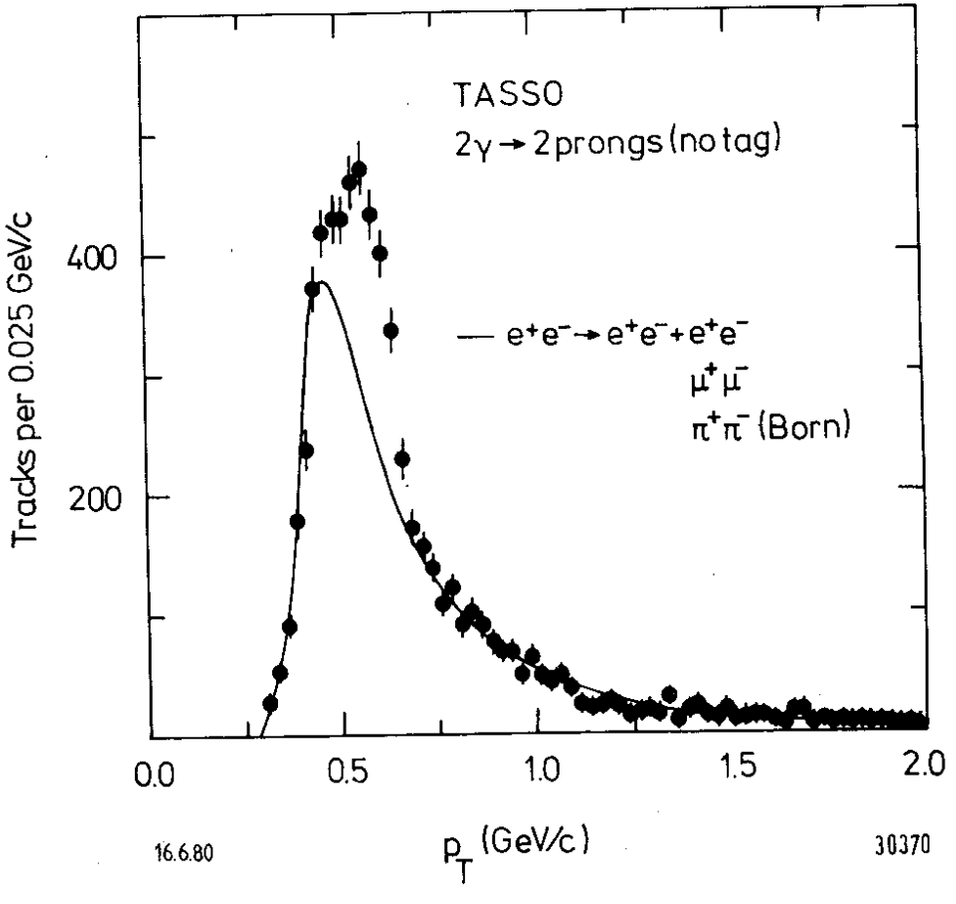
TASSO
2γ → 2 prongs (no tag)
Tracks per 0.025 GeV/c
400
200
— $e^+e^- \to e^+e^- + e^+e^-$
$\mu^+\mu^-$
$\pi^+\pi^-$ (Born)
0.0
0.5
1.0
1.5
2.0
16.6.80
p_T (GeV/c)
30370

Fig. 6

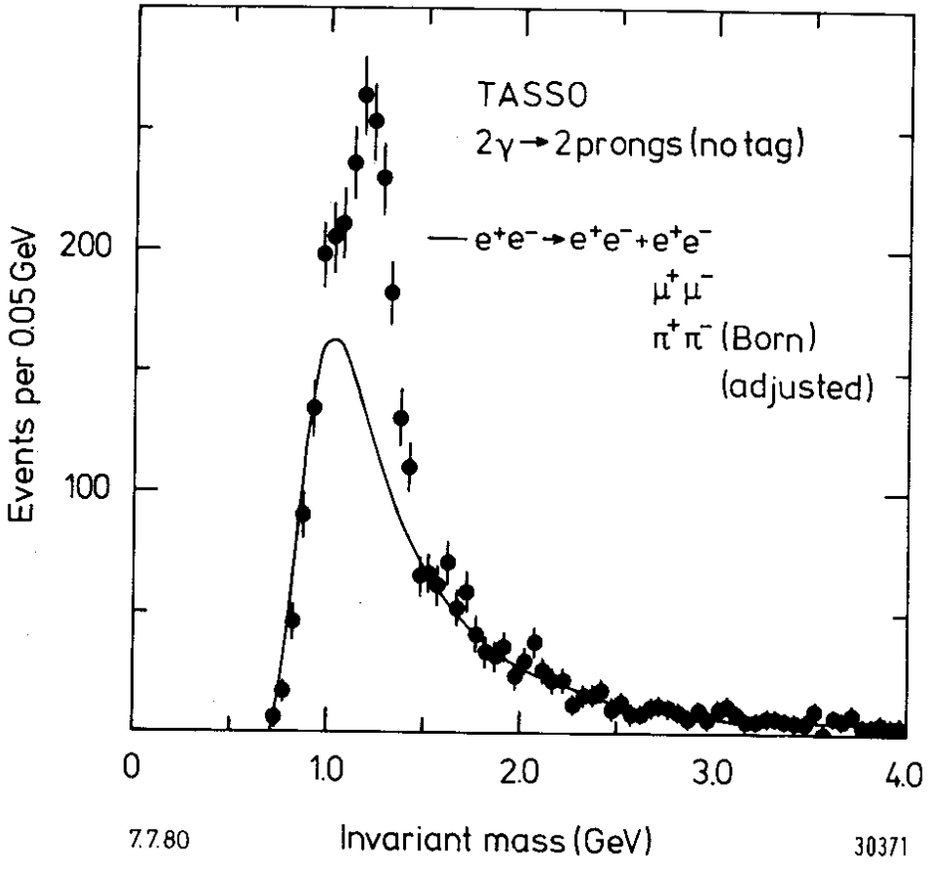
TASSO
2γ → 2 prongs (no tag)
— e⁺e⁻ → e⁺e⁻ + e⁺e⁻
μ⁺μ⁻
π⁺π⁻ (Born)
(adjusted)
Events per 0.05 GeV
200
100
0
1.0
2.0
3.0
4.0
7.7.80
Invariant mass (GeV)
30371

Fig. 7

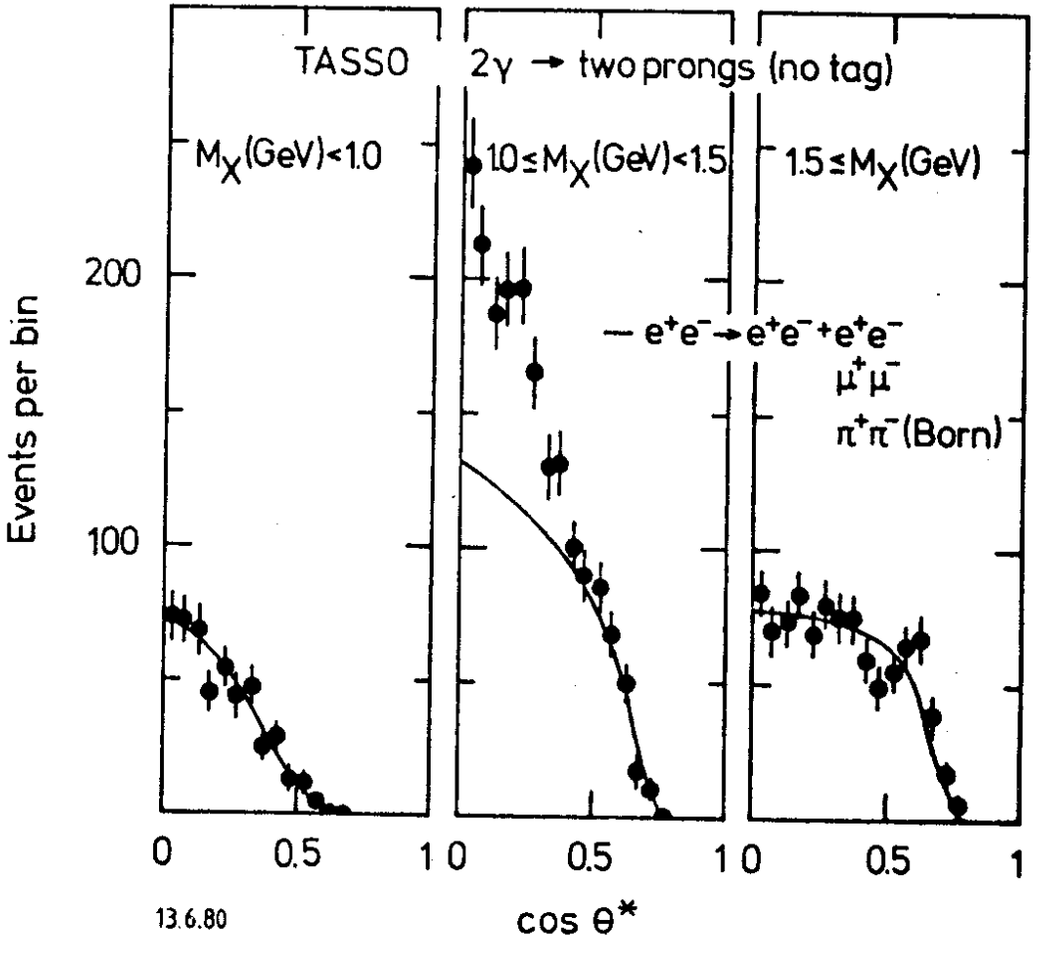
TASSO
2γ → two prongs (no tag)
M_X (GeV) < 1.0
1.0 ≤ M_X (GeV) < 1.5
1.5 ≤ M_X (GeV)
— e⁺e⁻ → e⁺e⁻ + e⁺e⁻
μ⁺μ⁻
π⁺π⁻ (Born)
Events per bin
200
100
0
0.5
1
13.6.80
cos θ*

Fig. 8

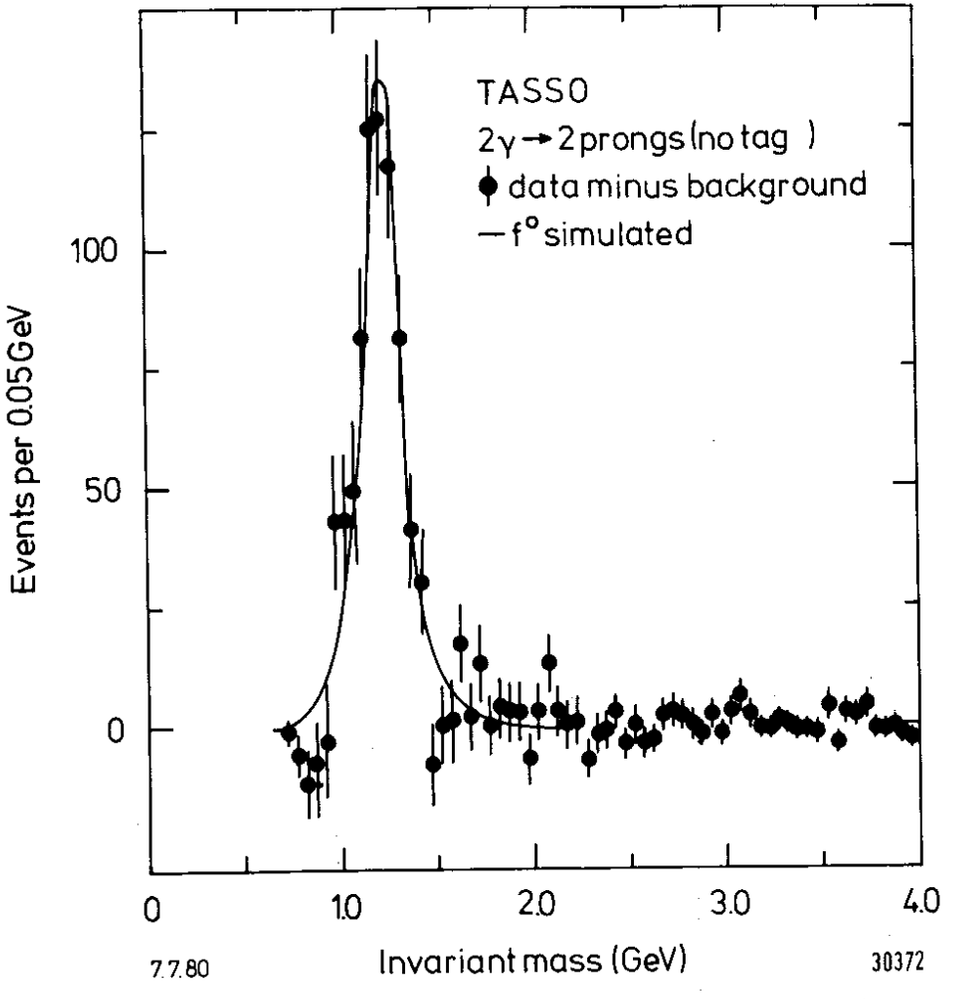
TASSO
2γ → 2 prongs (no tag)
data minus background
f° simulated
Events per 0.05 GeV
100
50
0
0
1.0
2.0
3.0
4.0
Invariant mass (GeV)
7.7.80
30372

Fig. 9

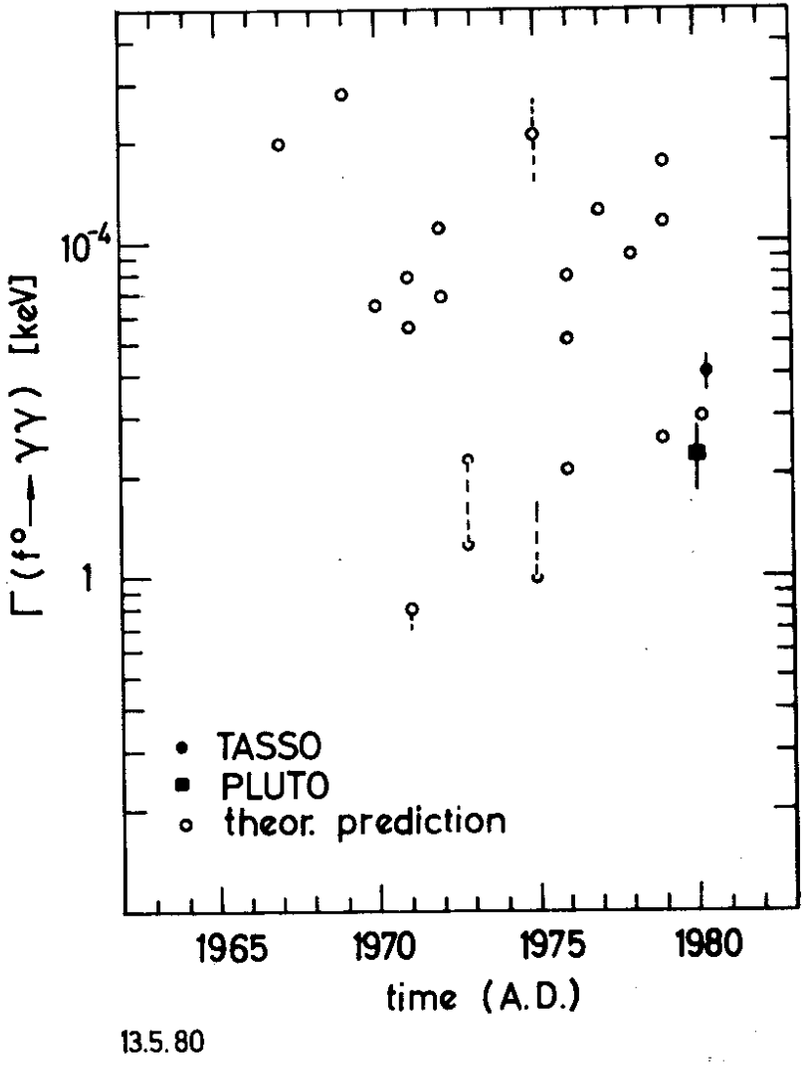
Γ (f° → γγ) [keV]
10⁻⁴
1
TASSO
PLUTO
theor. prediction
1965
1970
1975
1980
time (A.D.)
13.5.80

Fig. 10

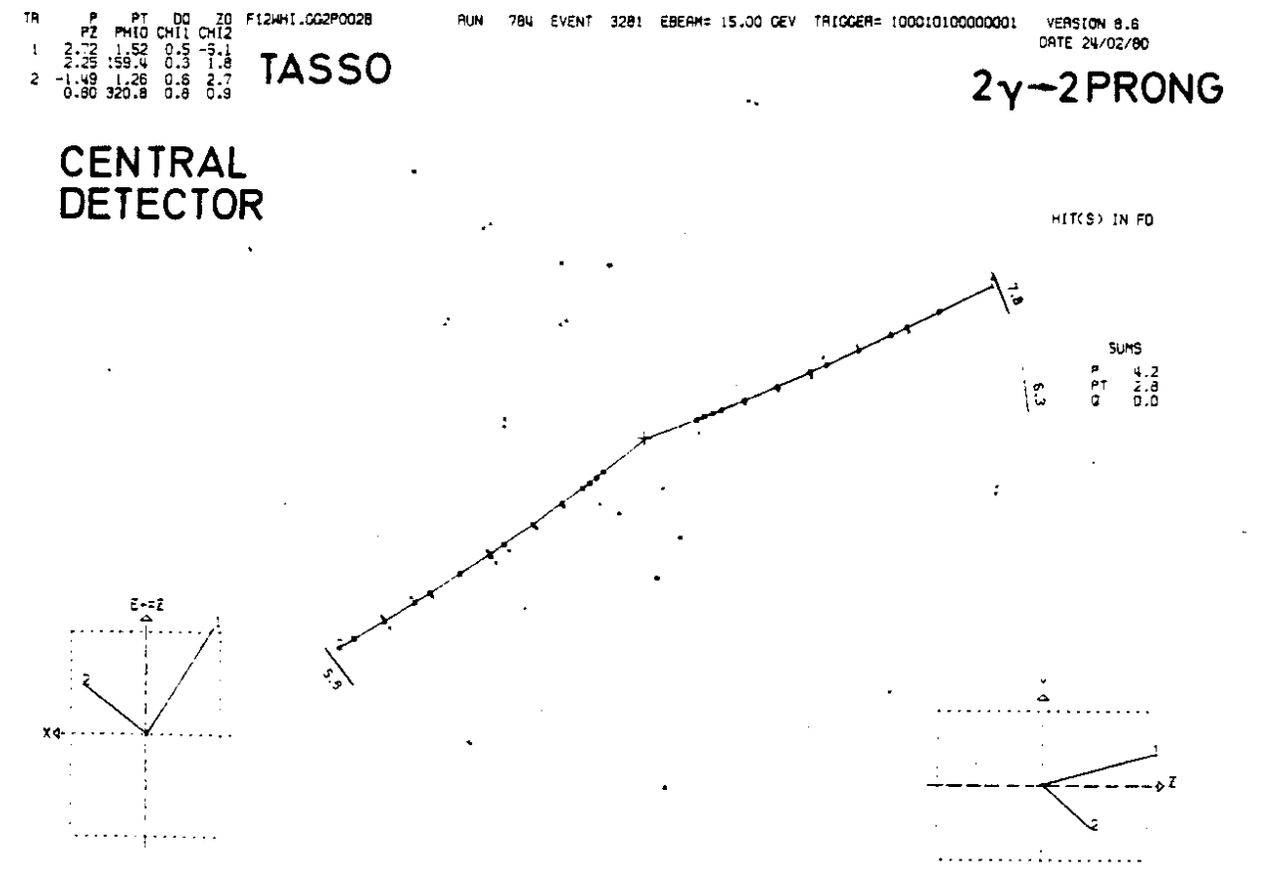
TR P PT DO Z0 F12WHI.GG2P002B RUN 784 EVENT 3281 EBEAM= 15.00 GEV TRIGGER= 1000101000000001 VERSION 8.6
PZ PHI0 CHI1 CHI2 DATE 24/02/80
1 2.72 1.52 0.5 -9.1
2.25 159.4 0.3 1.8
2 -1.49 1.26 0.6 2.7
0.80 320.8 0.8 0.9
TASSO
2γ–2 PRONG
CENTRAL DETECTOR
HIT(S) IN FD
SUMS
P 4.2
PT 2.8
Q 0.0
E=Z
XY
Z

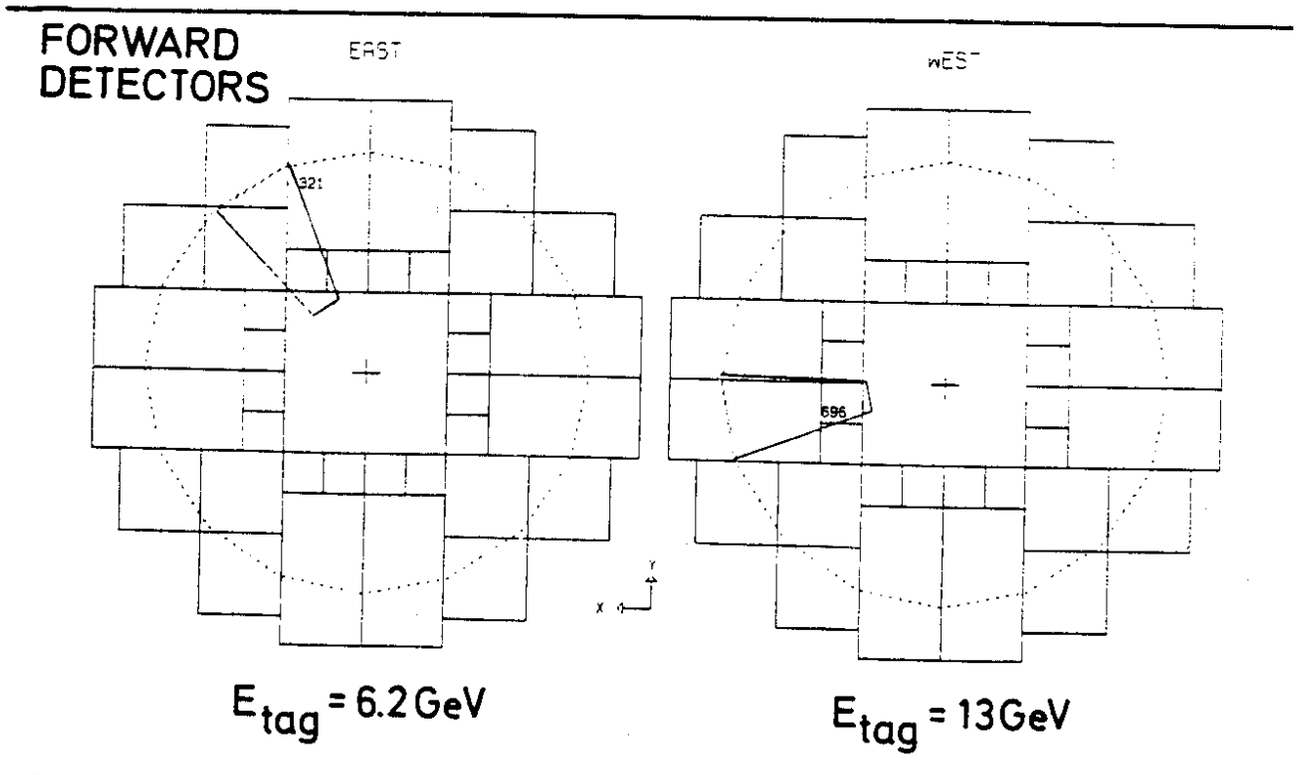
FORWARD DETECTORS
EAST
WEST
321
696
Etag = 6.2 GeV
Etag = 13 GeV

Fig. 11

21.4.80

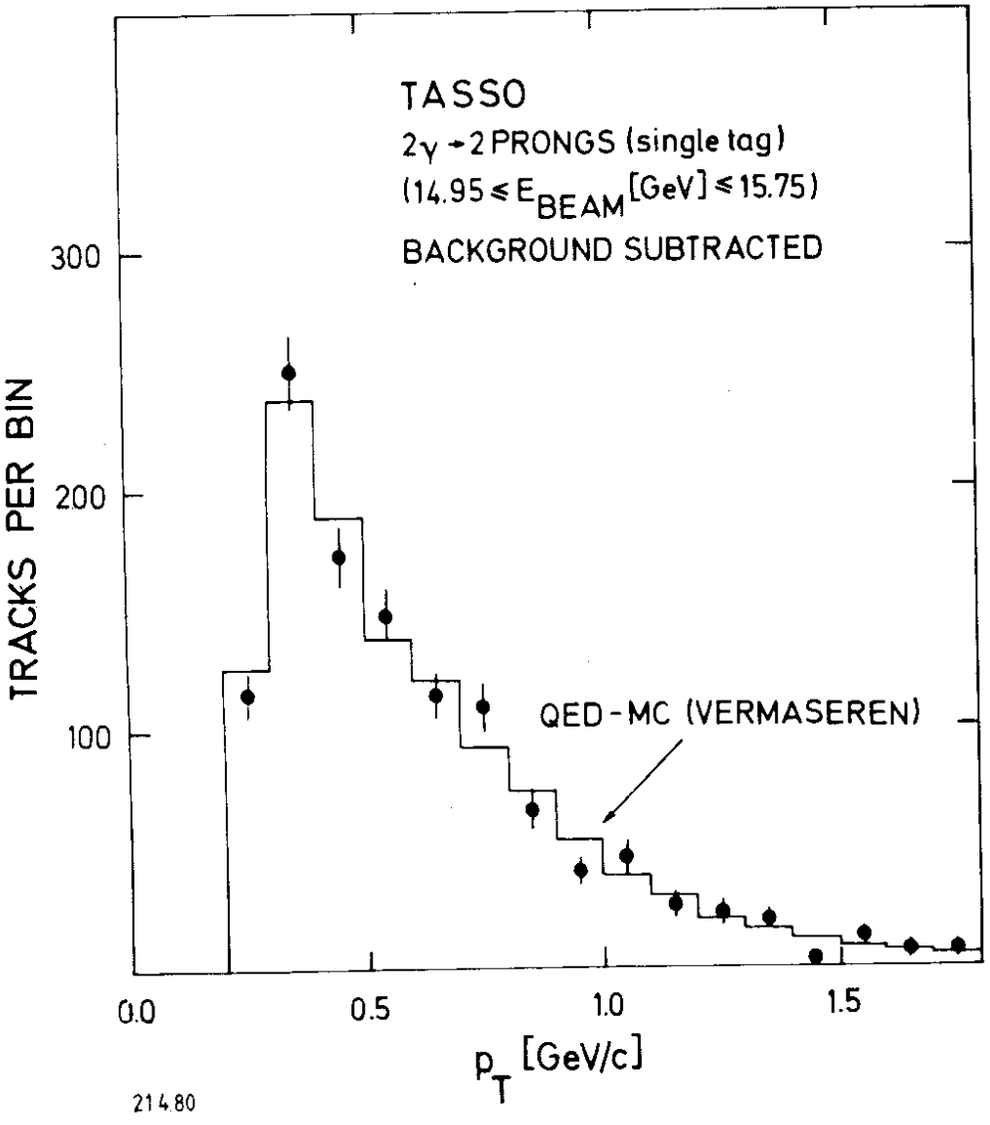

Fig. 12a

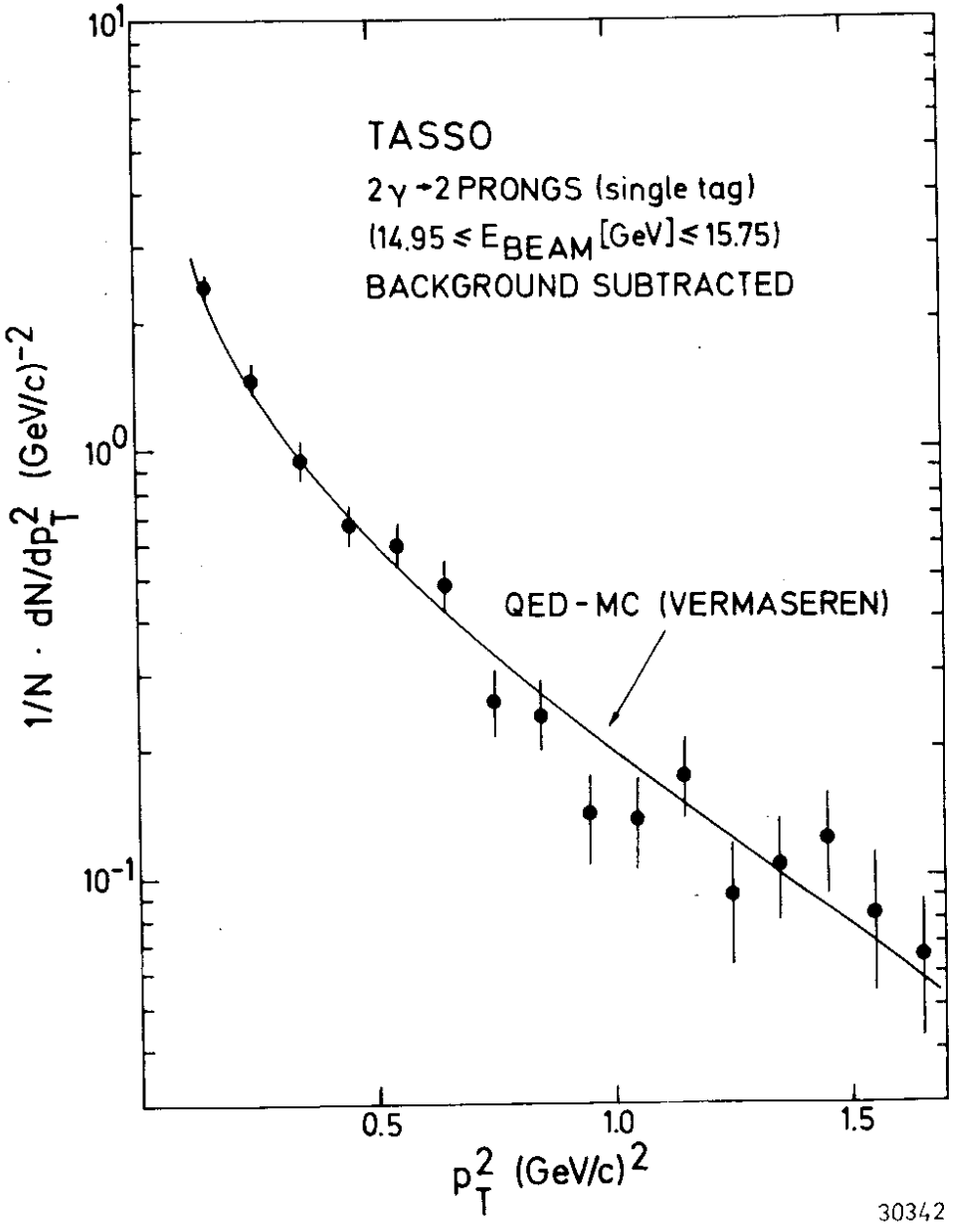

Fig. 12b

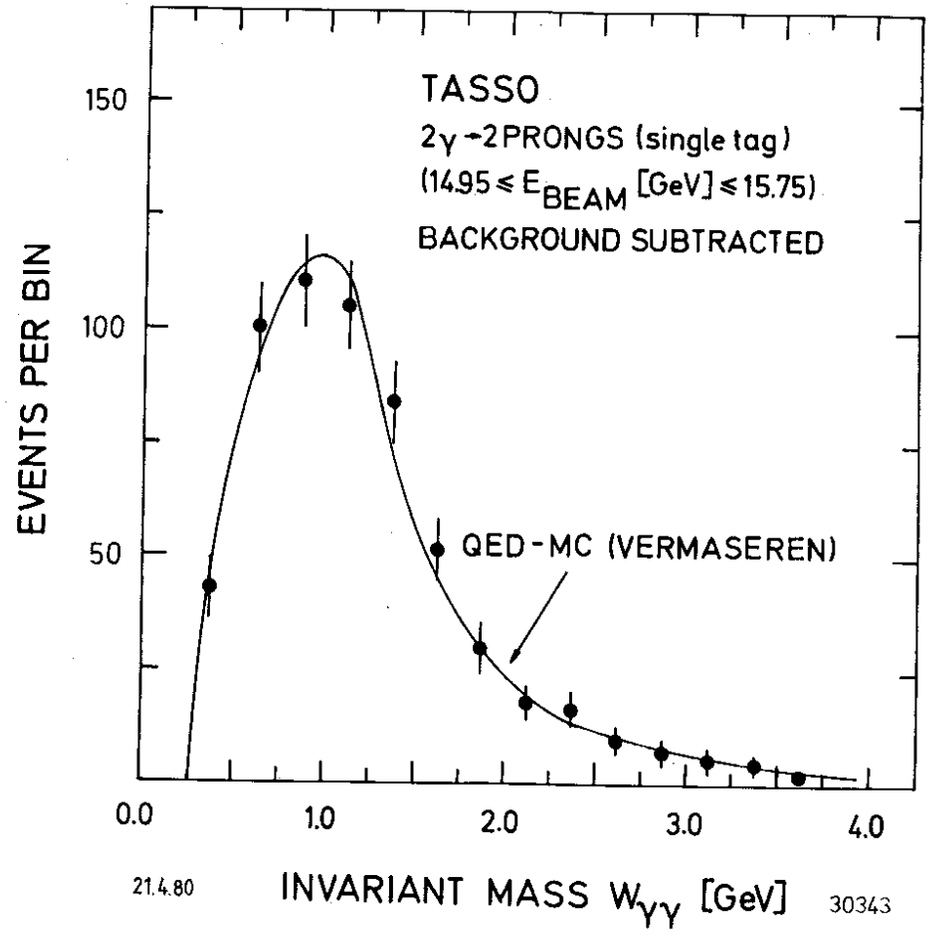
TASSO
2γ → 2 PRONGS (single tag)
(14.95 ≤ E_BEAM [GeV] ≤ 15.75)
BACKGROUND SUBTRACTED
QED - MC (VERMASEREN)
EVENTS PER BIN
150
100
50
0.0
1.0
2.0
3.0
4.0
21.4.80
INVARIANT MASS W_γγ [GeV]
30343

Fig. 13

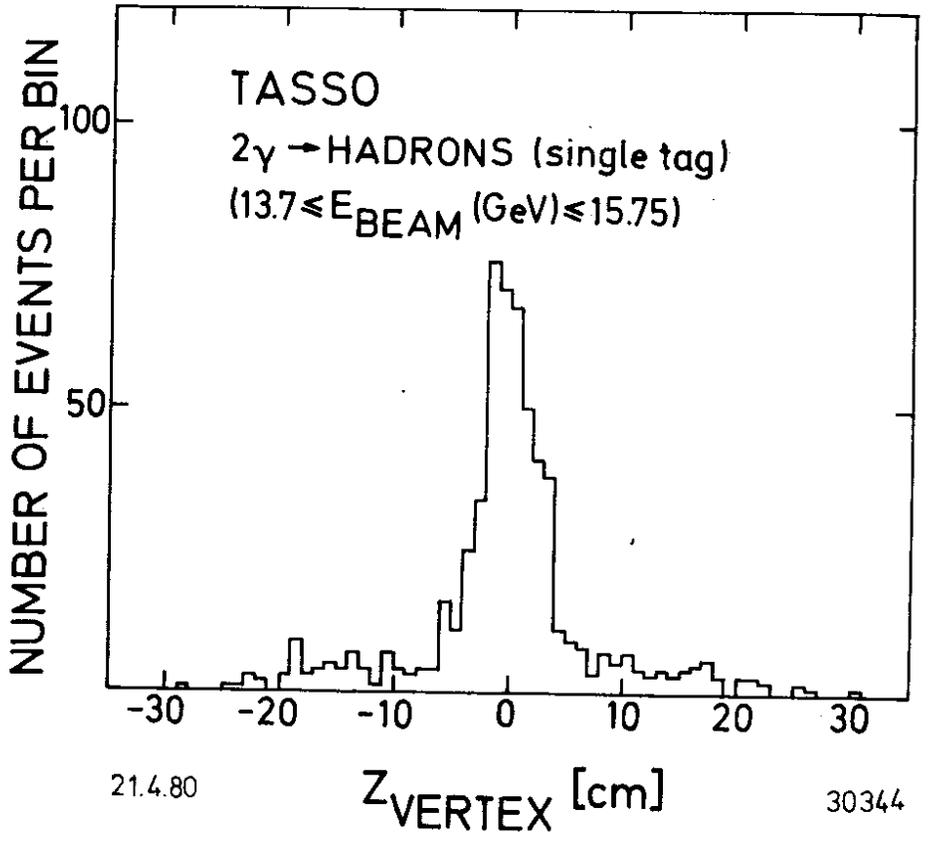
TASSO
2γ → HADRONS (single tag)
(13.7 ≤ E_BEAM (GeV) ≤ 15.75)
NUMBER OF EVENTS PER BIN
100
50
-30
-20
-10
0
10
20
30
21.4.80
Z_VERTEX [cm]
30344

Fig. 14

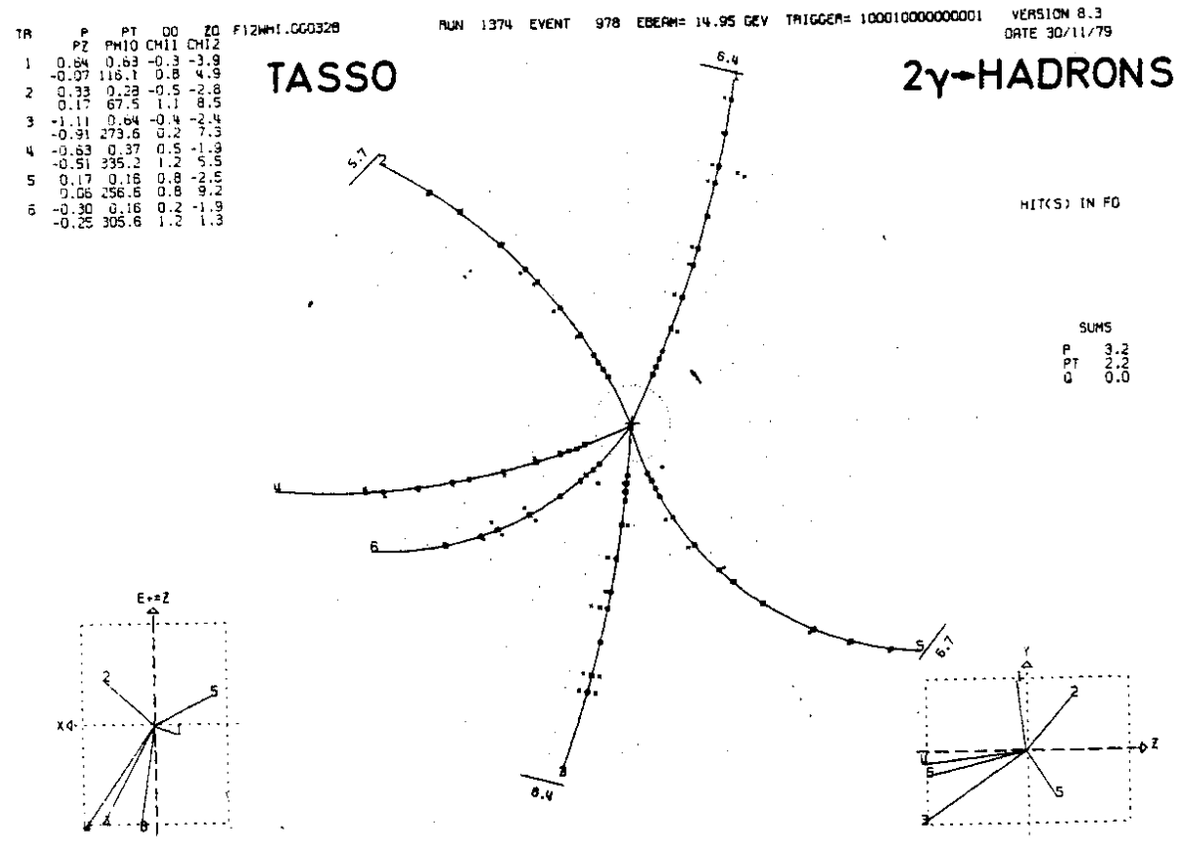

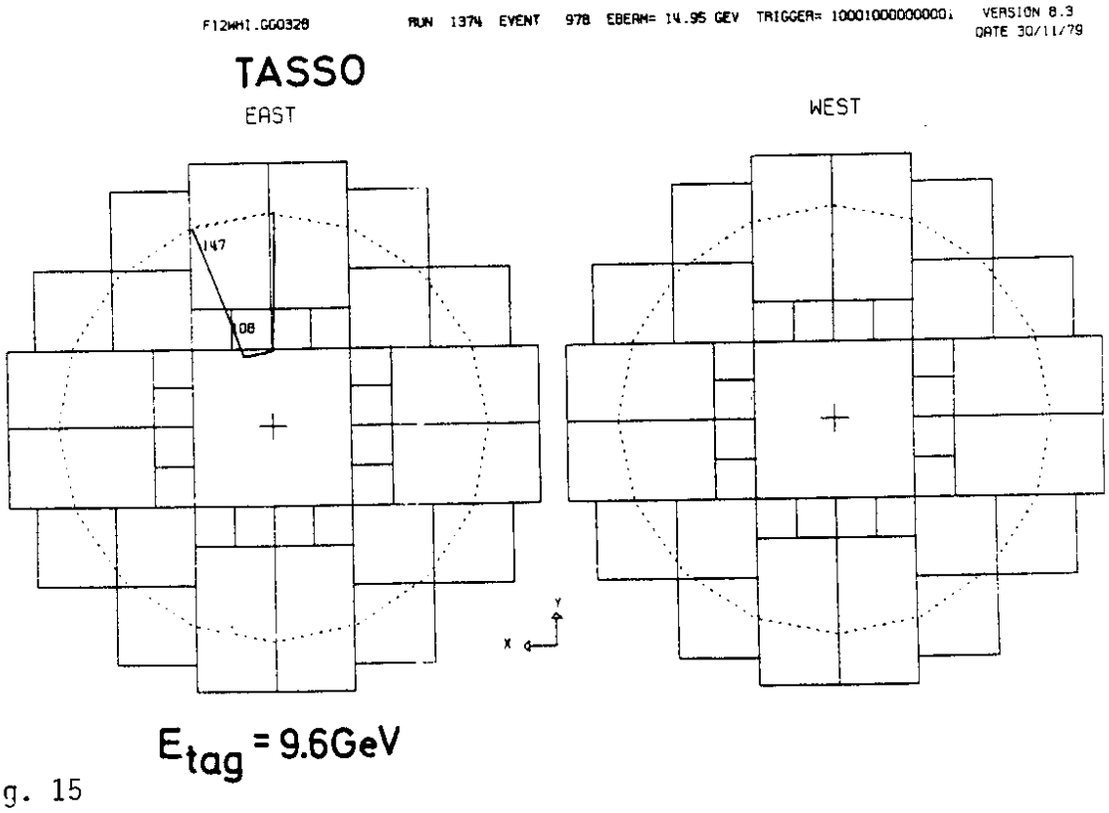

$E_{tag} = 9.6GeV$

Fig. 15

21.4.80

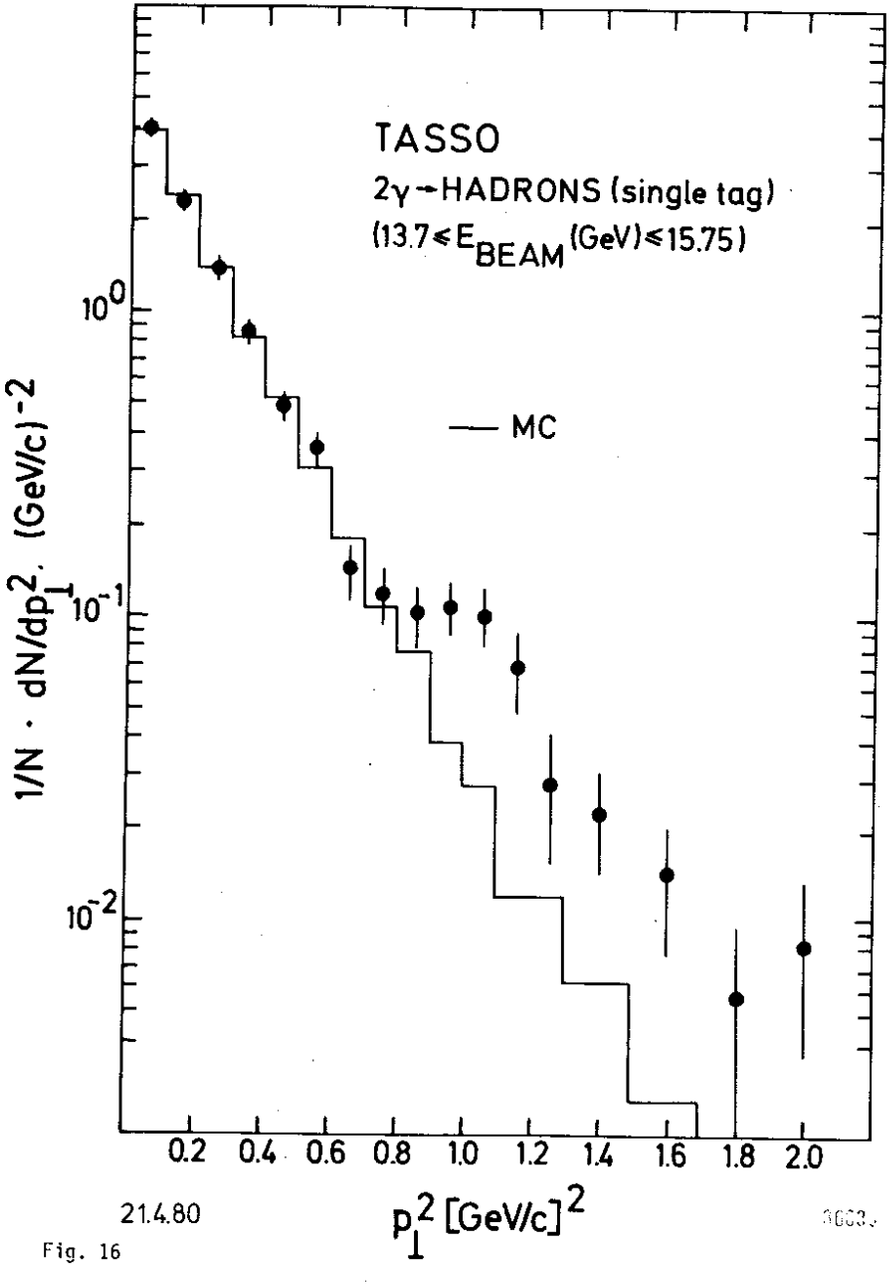
TASSO
2γ → HADRONS (single tag)
(13.7 ≤ E_BEAM (GeV) ≤ 15.75)
— MC
1/N · dN/dp²⊥ (GeV/c)⁻²
10⁰
10⁻¹
10⁻²
0.2 0.4 0.6 0.8 1.0 1.2 1.4 1.6 1.8 2.0
p²⊥ [GeV/c]²
21.4.80

Fig. 16

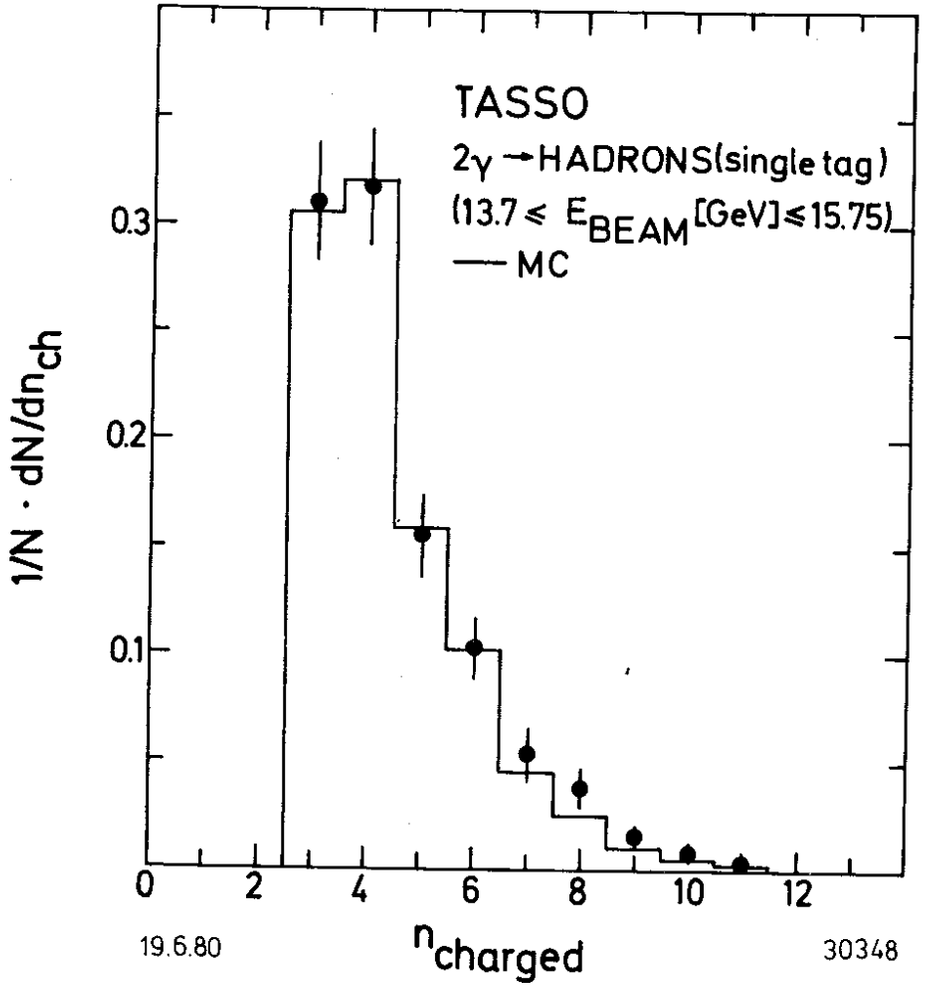
TASSO
2γ → HADRONS (single tag)
(13.7 ≤ E_BEAM [GeV] ≤ 15.75)
— MC
1/N · dN/dn_ch
0.3
0.2
0.1
0 2 4 6 8 10 12
n_charged
19.6.80
30348

Fig. 17

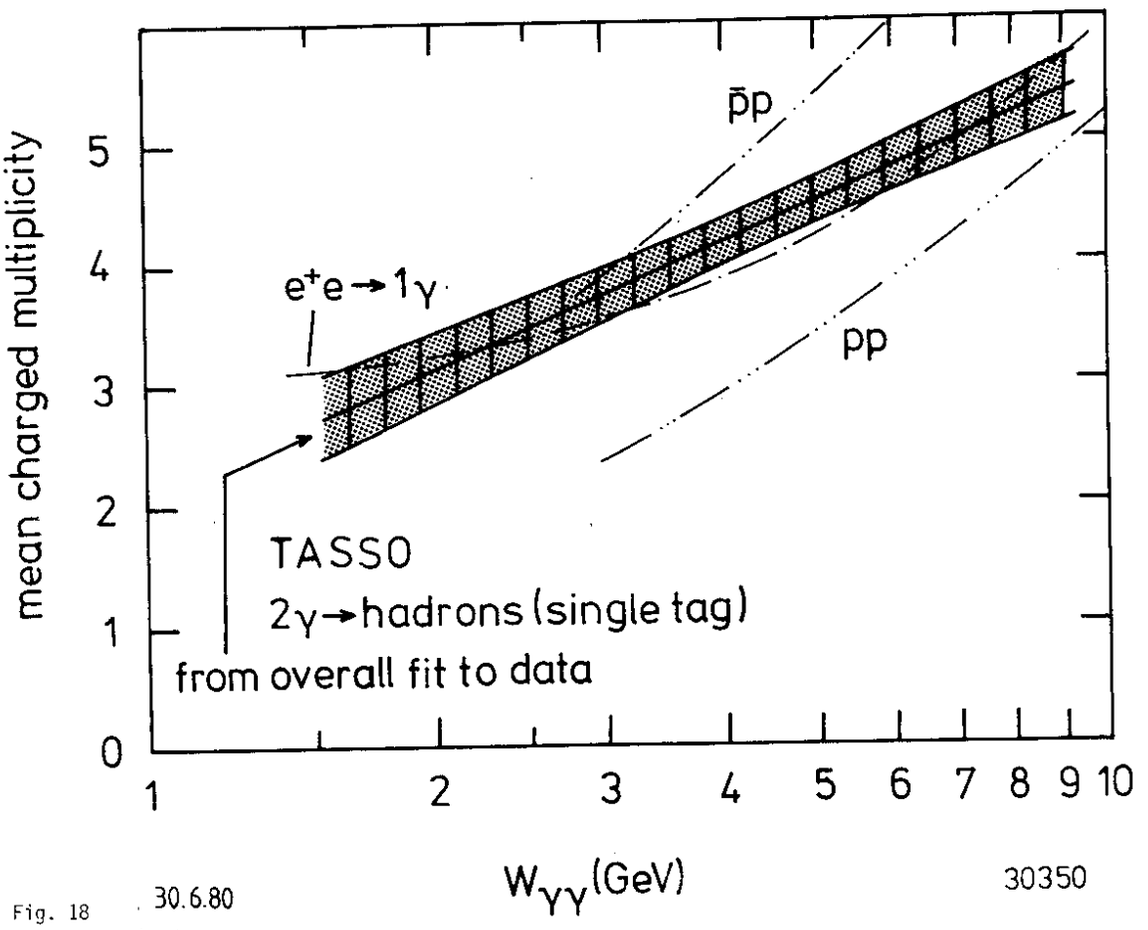
mean charged multiplicity
$\bar{p}p$
$e^+e \to 1\gamma$
pp
TASSO
$2\gamma \to$ hadrons (single tag)
from overall fit to data
$W_{\gamma\gamma}$(GeV)
30.6.80
30350

Fig. 18

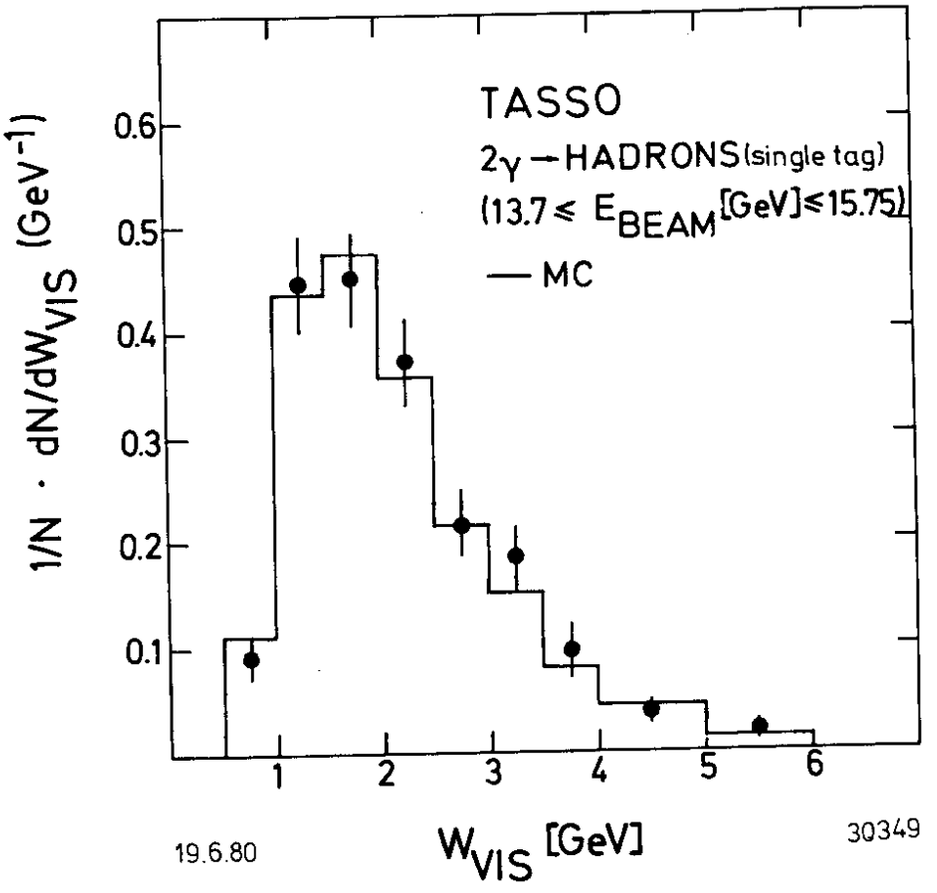
$1/N \cdot dN/dW_{VIS}$ (GeV^{-1})
TASSO
$2\gamma \to$ HADRONS (single tag)
$(13.7 \leq E_{BEAM}$ [GeV] $\leq 15.75)$
— MC
W_{VIS} [GeV]
19.6.80
30349

Fig. 19

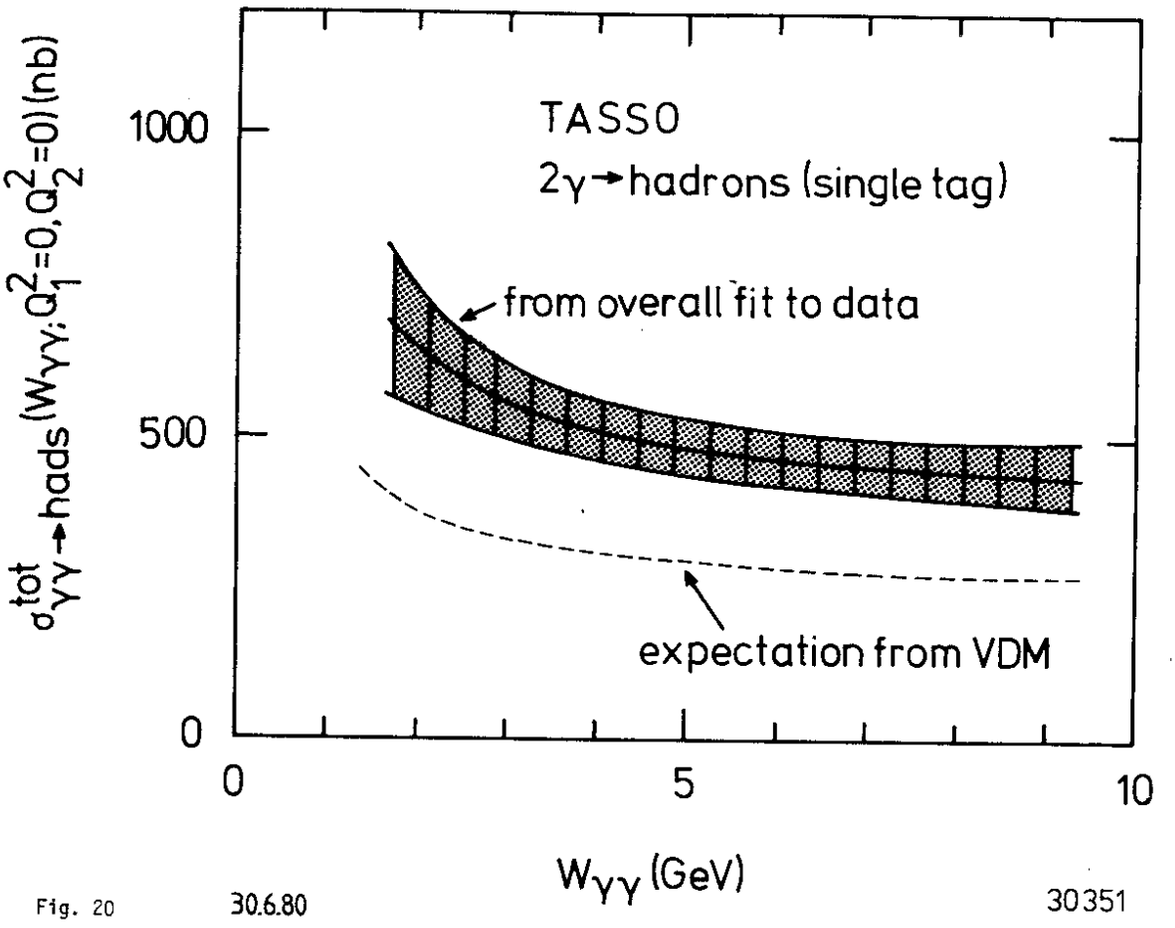

Fig. 20 30.6.80 30351